

Search for excited leptons in e^+e^- collisions at $\sqrt{s} = 161$ gev

P. Abreu, W. Adam, T. Adye, I. Azhinenko, G.D. Alekseev, R. Alemany, P.P. Allport, S. Almeded, U. Amaldi, S. Amato, et al.

► **To cite this version:**

P. Abreu, W. Adam, T. Adye, I. Azhinenko, G.D. Alekseev, et al.. Search for excited leptons in e^+e^- collisions at $\sqrt{s} = 161$ gev. Physics Letters B, Elsevier, 1997, 393, pp.245-260. in2p3-00007577

HAL Id: in2p3-00007577

<http://hal.in2p3.fr/in2p3-00007577>

Submitted on 26 Feb 1999

HAL is a multi-disciplinary open access archive for the deposit and dissemination of scientific research documents, whether they are published or not. The documents may come from teaching and research institutions in France or abroad, or from public or private research centers.

L'archive ouverte pluridisciplinaire **HAL**, est destinée au dépôt et à la diffusion de documents scientifiques de niveau recherche, publiés ou non, émanant des établissements d'enseignement et de recherche français ou étrangers, des laboratoires publics ou privés.

Search for excited leptons in e^+e^- collisions at $\sqrt{s} = 161$ GeV

DELPHI Collaboration

Abstract

A search with the DELPHI detector at LEP for excited leptons (e^* , μ^* , τ^* and ν^*) decaying through γ , W or Z transitions is reported. The data used correspond to an integrated luminosity of 10 pb^{-1} at an e^+e^- centre-of-mass energy of 161 GeV. The search for pair produced excited leptons established the limits $m_{e^*} > 79.6 \text{ GeV}/c^2$, $m_{\mu^*} > 79.6 \text{ GeV}/c^2$, $m_{\tau^*} > 79.4 \text{ GeV}/c^2$ and $m_{\nu^*} > 56.4 \text{ GeV}/c^2$ at 95% confidence level, assuming that the SU(2) and U(1) couplings of excited leptons are in the same ratio as for normal leptons and considering both left and right-handed components. Limits corresponding to other assumptions are also given. The search for single excited lepton production established upper limits on the ratio λ/m_{ℓ^*} of the coupling of the excited lepton to its mass.

(To be submitted to Physics Letters B)

P. Abreu²¹, W. Adam⁵⁰, T. Adye³⁷, I. Ajinenko⁴², G. D. Alekseev¹⁶, R. Alemany⁴⁹, P. P. Allport²², S. Almedhed²⁴, U. Amaldi⁹, S. Amato⁴⁷, A. Andreatza²⁸, M. L. Andrieux¹⁴, P. Antilogus⁹, W. D. Apel¹⁷, B. Åsman⁴⁴, J.-E. Augustin²⁵, A. Augustinus⁹, P. Baillon⁹, P. Bambade¹⁹, F. Barao²¹, R. Barate¹⁴, M. Barbi⁴⁷, D. Y. Bardin¹⁶, G. Barker⁹, A. Baroncelli⁴⁰, O. Barring²⁴, J. A. Barrio²⁶, W. Bartl⁵⁰, M. J. Bates³⁷, M. Battaglia¹⁵, M. Baubillier²³, J. Baudot³⁹, K.-H. Becks⁵², M. Begalli⁶, P. Beilliere⁸, Yu. Belokopytov^{9,53}, K. Belous⁴², A. C. Benvenuti⁵, M. Berggren⁴⁷, D. Bertini²⁵, D. Bertrand², M. Besancon³⁹, F. Bianchi⁴⁵, M. Bigi⁴⁵, M. S. Bilenky¹⁶, P. Billoir²³, M.-A. Bizouard¹⁹, D. Bloch¹⁰, M. Blume⁵², T. Bolognese³⁹, M. Bonesini²⁸, W. Bonivento²⁸, P. S. L. Booth²², G. Borisov^{39,42}, C. Bosio⁴⁰, O. Botner⁴⁸, E. Boudinov³¹, B. Bouquet¹⁹, C. Bourdarios⁹, T. J. V. Bowcock²², M. Bozzo¹³, P. Branchini⁴⁰, K. D. Brand³⁶, T. Brenke⁵², R. A. Brenner¹⁵, C. Bricman², R. C. A. Brown⁹, P. Bruckman¹⁸, J.-M. Brunet⁸, L. Bugge³³, T. Buran³³, T. Burgsmueller⁵², P. Buschmann⁵², S. Cabrera⁴⁹, M. Caccia²⁸, M. Calvi²⁸, A. J. Camacho Rozas⁴¹, T. Camporesi⁹, V. Canale³⁸, M. Canepa¹³, K. Cankocak⁴⁴, F. Cao², F. Carena⁹, L. Carroll²², C. Caso¹³, M. V. Castillo Gimenez⁴⁹, A. Cattai⁹, F. R. Cavallo⁵, V. Chabaud⁹, M. Chapkin⁴², Ph. Charpentier⁹, L. Chaussard²⁵, P. Checchia³⁶, G. A. Chelkov¹⁶, M. Chen², R. Chierici⁴⁵, P. Chliapnikov⁴², P. Chochula⁷, J. Chodoba³⁰, V. Chorowicz⁹, V. Cindro⁴³, P. Collins⁹, R. Contri¹³, E. Cortina⁴⁹, G. Cosme¹⁹, F. Cossutti⁴⁶, J.-H. Cowell²², H. B. Crawley¹, D. Crennell³⁷, G. Crosetti¹³, J. Cuevas Maestro³⁴, S. Czellar¹⁵, E. Dahl-Jensen²⁹, J. Dahm⁵², B. Dalmagne¹⁹, M. Dam²⁹, G. Damgaard²⁹, P. D. Dauncey³⁷, M. Davenport⁹, W. Da Silva²³, C. Defoix⁸, A. Deghorain², G. Della Ricca⁴⁶, P. Delpierre²⁷, N. Demaria³⁵, A. De Angelis⁹, W. De Boer¹⁷, S. De Brabandere², C. De Clercq², C. De La Vaissiere²³, B. De Lotto⁴⁶, A. De Min³⁶, L. De Paula⁴⁷, C. De Saint-Jean³⁹, H. Dijkstra⁹, L. Di Ciaccio³⁸, A. Di Diodato³⁸, F. Djama¹⁰, A. Djannati⁸, J. Dolbeau⁸, K. Doroba⁵¹, M. Dracos¹⁰, J. Drees⁵², K.-A. Drees⁵², M. Dris³², J.-D. Durand²⁵, D. Edsall¹, R. Ehret¹⁷, G. Eigen⁴, T. Ekelof⁴⁸, G. Ekspong⁴⁴, M. Elsing⁵², J.-P. Engel¹⁰, B. Erzen⁴³, M. Espirito Santo²¹, E. Falk²⁴, D. Fassouliotis³², M. Feindt⁹, A. Ferrer⁴⁹, S. Fichtel²³, T. A. Filippas³², A. Firestone¹, P.-A. Fischer¹⁰, H. Foeth⁹, E. Fokitis³², F. Fontanelli¹³, F. Formenti⁹, B. Franek³⁷, P. Frenkiel⁸, D. C. Fries¹⁷, A. G. Frodesen⁴, R. Fruhwirth⁵⁰, F. Fulda-Quenzer¹⁹, J. Fuster⁴⁹, A. Galloni²², D. Gamba⁴⁵, M. Gandelman⁴⁷, C. Garcia⁴⁹, J. Garcia⁴¹, C. Gaspar⁹, U. Gasparini³⁶, Ph. Gavellet⁹, E. N. Gazis³², D. Gele¹⁰, J.-P. Gerber¹⁰, L. Gerdyukov⁴², R. Gokheli⁵¹, B. Golob⁴³, G. Gopal³⁷, L. Gorn¹, M. Gorski⁵¹, Yu. Gouz^{45,53}, V. Gracco¹³, E. Graziani⁴⁰, C. Green²², A. Grefrath⁵², P. Gris³⁹, G. Grosdidier¹⁹, K. Grzelak⁵¹, S. Gumenyuk^{28,53}, P. Gunnarsson⁴⁴, M. Gunther⁴⁸, J. Guy³⁷, F. Hahn⁹, S. Hahn⁵², Z. Hajduk¹⁸, A. Hallgren⁴⁸, K. Hamacher⁵², F. J. Harris³⁵, V. Hedberg²⁴, R. Henriques²¹, J. J. Hernandez⁴⁹, P. Herquet², H. Heri⁹, T. L. Hessing³⁵, E. Higon⁴⁹, H. J. Hilke⁹, T. S. Hill¹, S.-O. Holmgren⁴⁴, P. J. Holt³⁵, D. Holthuisen³¹, S. Hoorelbeke², M. Houlden²², K. Huet³⁹, K. Hultqvist⁴⁴, J. N. Jackson²², R. Jacobsson⁴⁴, P. J. Jalocho¹⁸, R. Janik⁷, Ch. Jarlskog²⁴, G. Jarlskog²⁴, P. Jarry³⁹, B. Jean-Marie¹⁹, E. K. Johansson⁴⁴, L. Jonsson²⁴, P. Jonsson²⁴, C. Joram⁹, P. Juillot¹⁰, M. Kaiser¹⁷, F. Kapusta²³, K. Karafasoulis¹¹, M. Karlsson⁴⁴, E. Karvelas¹¹, S. Katsanevas³, E. C. Katsoufis³², R. Keranen⁴, Yu. Khokhlov⁴², B. A. Khomenko¹⁶, N. N. Khovanski¹⁶, B. King²², N. J. Kjaer³¹, O. Klapp⁵², H. Klein⁹, A. Klovning⁴, P. Kluit³¹, P. Kokkinias¹¹, A. Konopliannikov⁴², M. Koratzinos⁹, K. Korcyl¹⁸, V. Kostioukhine⁴², C. Kourkoumelis³, O. Kouznetsov^{13,16}, M. Krammer⁵⁰, C. Kreuter⁹, I. Kronkvist²⁴, Z. Krumstein¹⁶, W. Krupinski¹⁸, P. Kubinec⁷, W. Kucewicz¹⁸, K. Kurvinen¹⁵, C. Lacasta⁴⁹, I. Laktineh²⁵, J. W. Lamsa¹, L. Lancieri⁴⁶, D. W. Lane¹, P. Langefeld⁵², V. Lapin⁴², J.-P. Laugier³⁹, R. Lauhakangas¹⁵, G. Leder⁵⁰, F. Ledroit¹⁴, V. Lefebvre², C. K. Legan¹, R. Leitner³⁰, J. Lemonne², G. Lenzen⁵², V. Lepeltier¹⁹, T. Lesiak¹⁸, J. Libby³⁵, D. Liko⁹, R. Lindner⁵², A. Lipniacka⁴⁴, I. Lippi³⁶, B. Loerstad²⁴, J. G. Loken³⁵, J. M. Lopez⁴¹, D. Loukas¹¹, P. Lutz³⁹, L. Lyons³⁵, J. MacNaughton⁵⁰, G. Maehlum¹⁷, J. R. Mahon⁶, A. Maio²¹, T. G. M. Malmgren⁴⁴, V. Malychhev¹⁶, F. Mandl⁵⁰, J. Marco⁴¹, R. Marco⁴¹, B. Marechal⁴⁷, M. Margoni³⁶, J.-C. Marin⁹, C. Mariotti⁹, A. Markou¹¹, C. Martinez-Rivero⁴¹, F. Martinez-Vidal⁴⁹, S. Marti i Garcia²², J. Masik³⁰, F. Matorras⁴¹, C. Matteuzzi²⁸, G. Matthiae³⁸, M. Mazzucato³⁶, M. Mc Cubbin²², R. Mc Kay¹, R. Mc Nulty²², J. Medbo⁴⁸, M. Merk³¹, C. Meroni²⁸, S. Meyer¹⁷, W. T. Meyer¹, M. Michelotto³⁶, E. Migliore⁴⁵, L. Mirabito²⁵, W. A. Mitaroff⁵⁰, U. Mjoernmark²⁴, T. Moa⁴⁴, R. Moeller²⁹, K. Moenig⁹, M. R. Monge¹³, P. Morettini¹³, H. Mueller¹⁷, K. Muenich⁵², M. Mulders³¹, L. M. Mundim⁶, W. J. Murray³⁷, B. Muryn^{14,18}, G. Myatt³⁵, F. Naraghi¹⁴, F. L. Navarria⁵, S. Navas⁴⁹, K. Nawrocki⁵¹, P. Negri²⁸, W. Neumann⁵², N. Neumeister⁵⁰, R. Nicolaidou³, B. S. Nielsen²⁹, M. Nieuwenhuizen³¹, V. Nikolaenko¹⁰, P. Niss⁴⁴, A. Nomerotski³⁶, A. Normand³⁵, W. Oberschulte-Beckmann¹⁷, V. Obraztsov⁴², A. G. Olshevski¹⁶, A. Onofre²¹, R. Orava¹⁵, K. Osterberg¹⁵, A. Ouraou³⁹, P. Paganini¹⁹, M. Paganoni^{9,28}, P. Pages¹⁰, R. Pain²³, H. Palka¹⁸, Th. D. Papadopoulou³², K. Papageorgiou¹¹, L. Pape⁹, C. Parkes³⁵, F. Parodi¹³, A. Passeri⁴⁰, M. Pegoraro³⁶, L. Peralta²¹, H. Pernegger⁵⁰, M. Pernicka⁵⁰, A. Perrotta⁵, C. Petridou⁴⁶, A. Petrolini¹³, H. T. Phillips³⁷, G. Piana¹³, F. Pierre³⁹, M. Pimenta²¹, T. Podobnik⁴³, O. Podobrin⁹, M. E. Pol⁶, G. Polok¹⁸, P. Poropat⁴⁶, V. Pozdniakov¹⁶, P. Privitera³⁸, N. Pukhaeva¹⁶, A. Pullia²⁸, D. Radojicic³⁵, S. Ragazzi²⁸, H. Rahmani³², J. Rames¹², P. N. Ratoff²⁰, A. L. Read³³, M. Reale⁵², P. Rebecchi¹⁹, N. G. Redaelli²⁸, M. Regler⁵⁰, D. Reid⁹, P. B. Renton³⁵, L. K. Resvanis³, F. Richard¹⁹, J. Richardson²², J. Ridky¹², G. Rinaudo⁴⁵, I. Ripp³⁹, A. Romero⁴⁵, I. Roncagliolo¹³, P. Ronchese³⁶, L. Roos²³, E. I. Rosenberg¹, P. Roudeau¹⁹, T. Rovelli⁵, V. Ruhlmann-Kleider³⁹, A. Ruiz⁴¹, K. Rybicki¹⁸, H. Saarikko¹⁵, Y. Sacquin³⁹, A. Sadovsky¹⁶, O. Sahr¹⁴, G. Sajot¹⁴, J. Salt⁴⁹, J. Sanchez²⁶, M. Sannino¹³, M. Schimmelpfennig¹⁷, H. Schneider¹⁷, U. Schwickerath¹⁷, M. A. E. Schyns⁵², G. Sciolla⁴⁵, F. Scuri⁴⁶, P. Seager²⁰, Y. Sedykh¹⁶, A. M. Segar³⁵, A. Seitz¹⁷, R. Sekulin³⁷, L. Serbelloni³⁸, R. C. Shellard⁶, P. Siegrist³⁹, R. Silvestre³⁹, S. Simonetti³⁹, F. Simonetto³⁶, A. N. Sisakian¹⁶, B. Sitar⁷, T. B. Skaali³³, G. Smadja²⁵, N. Smirnov⁴², O. Smirnova²⁴, G. R. Smith³⁷, A. Sokolov⁴², R. Sosnowski⁵¹, D. Souza-Santos⁶, T. Spassov²¹, E. Spiriti⁴⁰, P. Sponholz⁵², S. Squarcia¹³, D. Stampfer⁹, C. Stanescu⁴⁰, S. Stanic⁴³, S. Stapnes³³, I. Stavitski³⁶, K. Stevenson³⁵, A. Stocchi¹⁹

J.Strauss⁵⁰, R.Strub¹⁰, B.Stugu⁴, M.Szczekowski⁵¹, M.Szeptycka⁵¹, T.Tabarelli²⁸, J.P.Tavernet²³, J.Thomas³⁵, A.Tilquin²⁷, J.Timmermans³¹, L.G.Tkatchev¹⁶, T.Todorov¹⁰, S.Todorova¹⁰, D.Z.Toet³¹, A.Tomaradze², B.Tome²¹, A.Tonazzo²⁸, L.Tortora⁴⁰, G.Transtromer²⁴, D.Treille⁹, G.Tristram⁸, A.Trombini¹⁹, C.Troncon²⁸, A.Tsirou⁹, M-L.Turluer³⁹, I.A.Tyapkin¹⁶, M.Tyndel³⁷, S.Tzamaras²², B.Ueberschaer⁵², O.Ullaland⁹, G.Valenti⁵, E.Vallazza⁹, C.Vander Velde², G.W.Van Apeldoorn³¹, P.Van Dam³¹, W.K.Van Doninck², J.Van Eldik³¹, A.Van Lysebetten², N.Vassilopoulos³⁵, G.Vegni²⁸, L.Ventura³⁶, W.Venus³⁷, F.Verbeure², M.Verlato³⁶, L.S.Vertogradov¹⁶, D.Vilanova³⁹, P.Vincent²⁵, L.Vitale⁴⁶, E.Vlasov⁴², A.S.Vodopyanov¹⁶, V.Vrba¹², H.Wahlen⁵², C.Walck⁴⁴, F.Waldner⁴⁶, M.Weierstall⁵², P.Weilhammer⁹, C.Weiser¹⁷, A.M.Wetherell⁹, D.Wicke⁵², J.H.Wickens², M.Wielers¹⁷, G.R.Wilkinson⁹, W.S.C.Williams³⁵, M.Winter¹⁰, M.Witek¹⁸, T.Wlodek¹⁹, K.Woschnagg⁴⁸, K.Yip³⁵, O.Yushchenko⁴², F.Zach²⁵, A.Zaitsev⁴², A.Zalewska⁹, P.Zalewski⁵¹, D.Zavrtanik⁴³, E.Zevgolatakis¹¹, N.I.Zimin¹⁶, M.Zito³⁹, D.Zontar⁴³, G.C.Zucchelli⁴⁴, G.Zumerle³⁶

¹Department of Physics and Astronomy, Iowa State University, Ames IA 50011-3160, USA

²Physics Department, Univ. Instelling Antwerpen, Universiteitsplein 1, B-2610 Wilrijk, Belgium and IIHE, ULB-VUB, Pleinlaan 2, B-1050 Brussels, Belgium

and Faculté des Sciences, Univ. de l'Etat Mons, Av. Maistriau 19, B-7000 Mons, Belgium

³Physics Laboratory, University of Athens, Solonos Str. 104, GR-10680 Athens, Greece

⁴Department of Physics, University of Bergen, Allégaten 55, N-5007 Bergen, Norway

⁵Dipartimento di Fisica, Università di Bologna and INFN, Via Irnerio 46, I-40126 Bologna, Italy

⁶Centro Brasileiro de Pesquisas Físicas, rua Xavier Sigaud 150, RJ-22290 Rio de Janeiro, Brazil and Depto. de Física, Pont. Univ. Católica, C.P. 38071 RJ-22453 Rio de Janeiro, Brazil

and Inst. de Física, Univ. Estadual do Rio de Janeiro, rua São Francisco Xavier 524, Rio de Janeiro, Brazil

⁷Comenius University, Faculty of Mathematics and Physics, Mlynska Dolina, SK-84215 Bratislava, Slovakia

⁸Collège de France, Lab. de Physique Corpusculaire, IN2P3-CNRS, F-75231 Paris Cedex 05, France

⁹CERN, CH-1211 Geneva 23, Switzerland

¹⁰Centre de Recherche Nucléaire, IN2P3 - CNRS/ULP - BP20, F-67037 Strasbourg Cedex, France

¹¹Institute of Nuclear Physics, N.C.S.R. Demokritos, P.O. Box 60228, GR-15310 Athens, Greece

¹²FZU, Inst. of Physics of the C.A.S. High Energy Physics Division, Na Slovance 2, 180 40, Praha 8, Czech Republic

¹³Dipartimento di Fisica, Università di Genova and INFN, Via Dodecaneso 33, I-16146 Genova, Italy

¹⁴Institut des Sciences Nucléaires, IN2P3-CNRS, Université de Grenoble 1, F-38026 Grenoble Cedex, France

¹⁵Research Institute for High Energy Physics, SEFT, P.O. Box 9, FIN-00014 Helsinki, Finland

¹⁶Joint Institute for Nuclear Research, Dubna, Head Post Office, P.O. Box 79, 101 000 Moscow, Russian Federation

¹⁷Institut für Experimentelle Kernphysik, Universität Karlsruhe, Postfach 6980, D-76128 Karlsruhe, Germany

¹⁸Institute of Nuclear Physics and University of Mining and Metallurgy, Ul. Kawiory 26a, PL-30055 Krakow, Poland

¹⁹Université de Paris-Sud, Lab. de l'Accélérateur Linéaire, IN2P3-CNRS, Bât. 200, F-91405 Orsay Cedex, France

²⁰School of Physics and Chemistry, University of Lancaster, Lancaster LA1 4YB, UK

²¹LIP, IST, FCUL - Av. Elias Garcia, 14-1º, P-1000 Lisboa Codex, Portugal

²²Department of Physics, University of Liverpool, P.O. Box 147, Liverpool L69 3BX, UK

²³LPNHE, IN2P3-CNRS, Universités Paris VI et VII, Tour 33 (RdC), 4 place Jussieu, F-75252 Paris Cedex 05, France

²⁴Department of Physics, University of Lund, Sölvegatan 14, S-22363 Lund, Sweden

²⁵Université Claude Bernard de Lyon, IPNL, IN2P3-CNRS, F-69622 Villeurbanne Cedex, France

²⁶Universidad Complutense, Avda. Complutense s/n, E-28040 Madrid, Spain

²⁷Univ. d'Aix - Marseille II - CPP, IN2P3-CNRS, F-13288 Marseille Cedex 09, France

²⁸Dipartimento di Fisica, Università di Milano and INFN, Via Celoria 16, I-20133 Milan, Italy

²⁹Niels Bohr Institute, Blegdamsvej 17, DK-2100 Copenhagen 0, Denmark

³⁰NC, Nuclear Centre of MFF, Charles University, Areal MFF, V Holesovickach 2, 180 00, Praha 8, Czech Republic

³¹NIKHEF, Postbus 41882, NL-1009 DB Amsterdam, The Netherlands

³²National Technical University, Physics Department, Zografou Campus, GR-15773 Athens, Greece

³³Physics Department, University of Oslo, Blindern, N-1000 Oslo 3, Norway

³⁴Dpto. Física, Univ. Oviedo, C/P. Pérez Casas, S/N-33006 Oviedo, Spain

³⁵Department of Physics, University of Oxford, Keble Road, Oxford OX1 3RH, UK

³⁶Dipartimento di Fisica, Università di Padova and INFN, Via Marzolo 8, I-35131 Padua, Italy

³⁷Rutherford Appleton Laboratory, Chilton, Didcot OX11 0QX, UK

³⁸Dipartimento di Fisica, Università di Roma II and INFN, Tor Vergata, I-00173 Rome, Italy

³⁹CEA, DAPNIA/Service de Physique des Particules, CE-Saclay, F-91191 Gif-sur-Yvette Cedex, France

⁴⁰Istituto Superiore di Sanità, Ist. Naz. di Fisica Nucl. (INFN), Viale Regina Elena 299, I-00161 Rome, Italy

⁴¹Instituto de Física de Cantabria (CSIC-UC), Avda. los Castros, S/N-39006 Santander, Spain, (CICYT-AEN93-0832)

⁴²Inst. for High Energy Physics, Serpukov P.O. Box 35, Protvino, (Moscow Region), Russian Federation

⁴³Department of Astroparticle Physics, School of Environmental Sciences, Nova Gorica, and J. Stefan Institute, Ljubljana, Slovenia

⁴⁴Fysikum, Stockholm University, Box 6730, S-113 85 Stockholm, Sweden

⁴⁵Dipartimento di Fisica Sperimentale, Università di Torino and INFN, Via P. Giuria 1, I-10125 Turin, Italy

⁴⁶Dipartimento di Fisica, Università di Trieste and INFN, Via A. Valerio 2, I-34127 Trieste, Italy

and Istituto di Fisica, Università di Udine, I-33100 Udine, Italy

⁴⁷Univ. Federal do Rio de Janeiro, C.P. 68528 Cidade Univ., Ilha do Fundão BR-21945-970 Rio de Janeiro, Brazil

⁴⁸Department of Radiation Sciences, University of Uppsala, P.O. Box 535, S-751 21 Uppsala, Sweden

⁴⁹IFIC, Valencia-CSIC, and D.F.A.M.N., U. de Valencia, Avda. Dr. Moliner 50, E-46100 Burjassot (Valencia), Spain

⁵⁰Institut für Hochenergiephysik, Österr. Akad. d. Wissensch., Nikolsdorfergasse 18, A-1050 Vienna, Austria

⁵¹Inst. Nuclear Studies and University of Warsaw, Ul. Hoza 69, PL-00681 Warsaw, Poland

⁵²Fachbereich Physik, University of Wuppertal, Postfach 100 127, D-42097 Wuppertal, Germany

⁵³On leave of absence from IHEP Serpukhov

1 Introduction

The recent increase in the centre-of-mass energy at LEP to $\sqrt{s} = 161$ GeV has opened up a new kinematic region for searches for “New Physics” going beyond the Standard Model (SM), including searches for excited states of leptons. Previous limits set by DELPHI and by other experiments can be found in references [1] and [2].

Excited leptons could be produced in pairs or singly, and would decay promptly to their ground state by radiating a γ , a Z , or a W [3], giving rise to different topologies. The partial decay width for each channel is a function of the excited lepton mass and of the coupling constants assumed in the model.

This paper presents a search for excited charged leptons (e^* , μ^* , and τ^*) and excited neutrinos (ν^*) in data taken by the DELPHI experiment at LEP and covers the $\gamma\gamma\nu\nu$, $ll\nu\nu$, $ll\gamma$, $ll\gamma\gamma$, $llll$, $l\nu$ jet jet, ll jet jet, $lll\nu$ jet jet and $l\nu\nu\nu$ jet jet final states. Analyses of photon production following reference [4], and of double photon production, are also reported. The data correspond to an integrated luminosity of 10 pb^{-1} at $\sqrt{s} = 161$ GeV.

2 Production and decay of excited leptons

Excited leptons (e^* , μ^* , τ^* and ν^*) are assumed to have spin and weak isospin $1/2$ and to be much heavier than the ordinary leptons. They can have left and right-handed components or only left-handed components, both cases will be considered. They are assumed to decay promptly, since for masses above 20 GeV their mean lifetime is predicted to be less than 10^{-15} seconds in all the cases studied.

2.1 Single production of excited leptons

In e^+e^- collisions, single excited leptons of the second (μ^* , ν_μ^*) and third (τ^* , ν_τ^*) family are produced through s -channel γ and Z exchanges, while in the first family (e^* , ν_e^*) there is an additional contribution due to t -channel exchanges [3,5] (W exchange in the case of ν_e^* , and γ and Z for e^*). In the t -channel, the spectator lepton is emitted preferentially at low polar angle and often goes undetected in the beam pipe.

The effective electroweak Lagrangian [5] associated to magnetic transitions from excited leptons ℓ^* to ordinary leptons ℓ has the form

$$L_{\ell\ell^*} = \frac{1}{2\Lambda} \bar{\ell}^* \sigma^{\mu\nu} \left[gf \frac{\tau}{2} W_{\mu\nu} + g' f' \frac{Y}{2} B_{\mu\nu} \right] \ell_L + h.c.$$

where Λ corresponds to the compositeness mass scale and the constants f and f' describe the effective changes from the SM coupling constants g and g' . The meaning of these couplings and of the other parameters is described in [5]. With the assumption $|f| = |f'|$, the cross section depends simply on the parameter f/Λ , which is related to the excited lepton mass according to $f/\Lambda = \sqrt{2}\lambda/m_{\ell^*}$, where λ is the coupling of the excited lepton.

2.2 Double production of excited leptons

The double production of charged excited leptons proceeds via s -channel γ and Z exchanges, while for excited neutrinos only the s -channel Z exchange contributes. Although t -channel contributions are also possible, they correspond to double de-excitation, and give a negligible contribution to the overall production cross-section [5]. Form factors

and anomalous magnetic moments of excited leptons are not considered in the present analysis. At LEP, double production of excited leptons with masses almost up to the beam energy can be detected.

2.3 Decay modes of excited leptons

Excited leptons can decay by radiating a γ , a Z , or a W . The decay branching ratios are functions of the f and f' coupling parameters of the model. Table 1 shows the branching ratios for some relevant values of f , f' , and the excited lepton mass.

Decay Channel	M=80 GeV/ c^2		M=160 GeV/ c^2	
	$f = f'$	$f = -f'$	$f = f'$	$f = -f'$
$\ell^* \rightarrow \ell\gamma$	100.0	0.0	38.6	0.0
$\ell^* \rightarrow \ell Z$	0.0	0.0	8.4	35.3
$\ell^* \rightarrow \nu W$	0.0	100.0	53.0	64.7
$\nu^* \rightarrow \nu\gamma$	0.0	100.0	0.0	38.6
$\nu^* \rightarrow \nu Z$	0.0	0.0	35.3	8.4
$\nu^* \rightarrow \ell W$	100.0	0.0	64.7	53.0

Table 1: Branching ratios in % for excited lepton decays (upper part for excited charged leptons, lower part for excited neutrinos).

For charged excited leptons, the electromagnetic radiative decay is forbidden if $f = -f'$, and the decay then proceeds via three body decay modes through the Z and W boson. But if $f = +f'$, the electromagnetic radiative decay branching ratio is close to 100% for m_{ℓ^*} below m_Z and m_W , and decreases only to 38% for $m_{\ell^*} = 160$ GeV/ c^2 .

For excited neutrinos, the situation is reversed, so that the electromagnetic partial decay width is zero if $f = +f'$. However, there is a significant contribution to the total decay width from the electromagnetic radiative decay if $f \neq f'$, even if the difference $f - f'$ is much smaller than f itself.

3 The DELPHI detector and the data samples

A detailed description of the DELPHI apparatus and its performance can be found in [6]. This analysis relies both on the charged particle detection provided by the tracking system and the neutral cluster detection provided by the electromagnetic and hadronic calorimeters.

The main tracking detector is the Time Projection Chamber (TPC), which covers the angular range $20^\circ < \theta < 160^\circ$, where θ is the polar angle defined with respect to the beam direction. Other detectors contributing to the track reconstruction are the Vertex Detector (VD), the Inner and Outer Detectors, the Forward Chambers, and the Muon Chambers. The best momentum resolution obtained for muons is $\sigma(1/p) = 0.57 \times 10^{-3}$ (GeV/ c) $^{-1}$.

The barrel electromagnetic calorimeter (HPC) and the forward electromagnetic calorimeters (FEMC and STIC) are used for the reconstruction of electromagnetic showers. The STIC (Small angle Tile Calorimeter), which is the DELPHI luminosity mon-

itor, was used for electromagnetic shower detection at very low polar angle and has an energy resolution of 2.7% for 45 GeV electrons. The energy resolutions of the HPC (High density Projection Chamber) and FEMC (Forward Electromagnetic Calorimeter) calorimeters are parameterized respectively as $\sigma(E)/E = 0.043 \oplus 0.32/\sqrt{E}$ and $\sigma(E)/E = 0.03 \oplus 0.12/\sqrt{E} \oplus 0.11/E$, where E is expressed in GeV and the symbol ‘ \oplus ’ implies addition in quadrature. The hadron calorimeter covers both the barrel and forward regions. It has an energy resolution of $\sigma(E)/E = 0.21 \oplus 1.12/\sqrt{E}$ in the barrel and about $2/\sqrt{E}$ in the forward region.

The effects of the experimental resolution, both on the signals and on the backgrounds, were studied by generating Monte Carlo events for the SM background processes and for the possible signals and passing them through the full DELPHI simulation and reconstruction chain.

Bhabha events, $e^+e^- \rightarrow Z\gamma$, $e^+e^- \rightarrow Zee$, $e^+e^- \rightarrow We\nu$, and $e^+e^- \rightarrow WW$ events were generated with PYTHIA [7]. EXCALIBUR [8] was also used to generate $e^+e^- \rightarrow We\nu$ and $Z\nu\nu$ events. The two-photon (“ $\gamma\gamma$ ”) physics events were generated according to the TWOGAM [9] generator for quark channels and the Berends, Daverveldt and Kleiss generator [10] for the electron, muon and tau channels. Compton events were generated according to [11], and $e^+e^- \rightarrow \gamma\gamma$ events according to [12].

Single and double excited lepton events were generated according to their cross-sections defined in [5] involving γ and Z exchange. The hadronization and decay processes were simulated by JETSET 7.4 [7]. The initial state radiation effect was included at the level of the generator for the single production, while for the double production it was taken into account in the total cross section. All the possible decays, $\ell^* \rightarrow \ell\gamma$, $\ell^* \rightarrow \nu W$, $\ell^* \rightarrow \ell Z$, $\nu^* \rightarrow \nu\gamma$, and $\nu^* \rightarrow \ell W$ [5], were included in the generator.

4 Data pre-selection and event classification

The final states of excited leptons at $\sqrt{s} = 161$ GeV are quite diverse and involve isolated photons, isolated leptons, jets, missing energy, and missing momentum. However, as excited leptons are produced almost at rest near the kinematic limit and their decays give at least one visible particle, all their decay modes can be characterized by a significant energy deposition in the central region of the detector. The “ $\gamma\gamma$ ” background was therefore drastically suppressed by requiring a visible energy greater than $0.2\sqrt{s}$ in the polar angle region between 20° and 160° , including at least one particle with an energy greater than 5 GeV. To be considered, a charged particle had to have a momentum greater than 0.4 GeV/ c , a polar angle between 20° and 160° , and a track length greater than 30 cm. In the central region ($40^\circ < \theta < 140^\circ$), the impact parameters in the transverse plane and in the beam direction had to be below 5 cm and 10 cm respectively. These values were increased to 10 cm and 20 cm in the forward region ($20^\circ < \theta < 40^\circ$ or $140^\circ < \theta < 160^\circ$). Events with measured charged or neutral particles having energy greater than \sqrt{s} were rejected.

After this pre-selection, the search for excited leptons was split between two classes of events. In searches in events with more than eight charged particles, the W or Z was assumed to have decayed hadronically. In searches in events with eight charged particles or less, the W or Z decay was assumed to have been leptonic, so that all the particles either were leptons or resulted from tau decay or from electron showers. In this way, the events were classified as *hadronic* or *leptonic*. Electromagnetic radiative decays of excited leptons were searched for in the *leptonic* events, which included purely photonic events.

Isolated leptons or photons were selected by requiring an energetic particle (jet or neutral cluster) separated from any significant nearby energy deposition.

Neutral clusters were considered to be isolated photons if, in a double cone centred in the cluster and having internal and external half angles of 5° and 15° , the total energy deposited was less than 1 GeV. Inside the inner cone, all the clusters were considered associated and no charged particles were allowed. Isolated clusters were also required to have an energy greater than 5 GeV. No recovery of converted photons was attempted.

In a similar way, charged particles were considered isolated if, in a double cone centred on their track with internal and external half angles of 3° and 15° , the total energy deposited was less than 1 GeV. Inside the inner cone, all the clusters and tracks were considered to be associated, and the total energy had to be greater than 5 GeV.

4.1 Selected *hadronic* events

In the topologies studied, excited lepton candidates classified as *hadronic* events should have two jets in the final state (from the W or Z decay). In these events, charged particles and neutral clusters not associated to charged particles were therefore clustered into two jets using the Durham jet algorithm [13].

In this algorithm, a resolution variable

$$y_{ij} = 2 \min(E_i^2, E_j^2) / E_{vis}^2 \cdot (1 - \cos \theta_{ij})$$

is computed for all pairs of particles, where $E_{i,j}$ are their energies, θ_{ij} is their opening angle, and E_{vis} is the visible energy in the event. The pair for which y_{ij} is smallest is replaced by a pseudoparticle with four-momentum equal to the sum of their four-momenta. The procedure is iterated until all the particles are clustered into two jets.

The value of the resolution variable in the last iteration, ie the value y_{cut23} at the transition between the clustering into three and two jets, was saved to allow a better characterization of the event topology. Events with high y_{cut23} have a topology with at least three jets.

Jets were called charged if they contained at least one charged particle. Only charged jets were retained.

4.2 Selected *leptonic* events

Excited lepton candidates classified as *leptonic* events can have muons, electrons or taus in the final state. Taus can decay into several charged and neutral particles. Electrons, due to interactions with matter, can be accompanied by other electrons and photons. Therefore the analysis was again based on the Durham jet algorithm [13], which was applied to all charged and neutral particles not associated to isolated photons. The cut-off parameter was set to $y_{cut} = 0.003$ to optimize the efficiency for the signal. However, to avoid clustering several isolated leptons in the same jet, the number of jets was forced to be at least equal to the number of isolated charged particles found previously.

5 Selected event topologies

The most relevant topologies for excited lepton searches are discussed in this section, both for *hadronic* and *leptonic* events.

In *hadronic* events from excited lepton production, the jets originate from the decay of a W or a Z which is not produced at rest. The candidates must have two charged jets

with high acollinearity (A_{col}) and acoplanarity (A_{cop})[†], and the two-jet system must have a high mass (M_{jj}) and a high momentum (P_{jj}). Events where the cut-off variable y_{cut23} , defined in section 4.1, was greater than 0.06 were rejected, to avoid topologies with more than two well defined jets.

The main background for *hadronic* events comes from radiative returns to the Z ($e^+e^- \rightarrow Z\gamma$) where the photon was lost in the beam pipe, which are characterized by a high missing momentum at very low polar angles. The WW contamination is small, and is characterised at this energy by the production of the W bosons nearly at rest.

In *leptonic* events, the main background comes from radiative leptonic events and from Compton events [14]. In topologies where the photon(s) are detected, cuts on the energy, isolation angle, and polar angle of the photon(s) can reduce the backgrounds drastically.

In all topologies, jets had to have a polar angle between 20° and 160° and the leading charged particle in the jet had to have a momentum above $1 \text{ GeV}/c$. The missing momentum and the missing energy were calculated using all the detected particles, including those in the very forward region (using the STIC information). Except for the purely photonic events, discussed in Section 5.6, the trigger efficiency was very close to 100%.

The results in all the channels described below are summarised in Tables 2 and 3, and discussed in Section 6.

5.1 Hadronic events with no isolated charged particles

Hadronic events with no isolated charged particles ($h200$ topology in Tables 2 and 3) can result from single production of excited leptons in the modes $l\ell^* \rightarrow l\nu W \rightarrow (\ell)\nu q_i q_j$ and $\nu\nu^* \rightarrow \nu\ell W \rightarrow \nu(\ell)q_i q_j$, where in both cases the final charged lepton (ℓ) was undetected (lost in the beam pipe or having insufficient momentum to be selected), and in the mode $\nu\nu^* \rightarrow \nu\nu Z \rightarrow \nu\nu q_i q_i$.

The specific selection criteria were that:

- the acollinearity and acoplanarity angles A_{col} and A_{cop} between the jets had to exceed 50° and 25° respectively,
- the polar angle of the missing momentum was required to be between 25° and 155° to reject radiative returns to the Z , and
- the invariant mass of the two-jet system had to exceed $40 \text{ GeV}/c^2$.

The corresponding distributions are shown in Fig. 1, together with a typical $\nu\nu^* \rightarrow \nu\nu Z \rightarrow \nu\nu q_i q_i$ signal simulation.

Two events passed these criteria, while 5.1 ± 0.5 were expected from the SM background. The main contributions to this background come from $q\bar{q}(\gamma)$ (4 events) and $W e\nu$ (1 event from EXCALIBUR or 0.4 from PYTHIA).

5.2 Hadronic events with one isolated charged particle

Hadronic events with one isolated charged particle ($h210$ topology) can be good candidates for single and double production of excited leptons.

5.2.1 Single production

In single production, the relevant modes are $l\ell^* \rightarrow l\nu W \rightarrow l\nu q_i q_j$, $\nu\nu^* \rightarrow \nu\ell W \rightarrow \nu\ell q_i q_j$, and $l\ell^* \rightarrow l\ell Z \rightarrow (\ell)\ell q_i q_j$ with one of the final charged leptons (ℓ) undetected (lost in the beam pipe or with momentum too low to be selected).

[†]The acoplanarity is defined as the acollinearity in the plane perpendicular to the beam.

The specific selection criteria were that:

- the polar angle of the isolated particle was required to be between 20° and 160° ,
- the angles A_{col} and A_{cop} between the jets had to exceed 30° and 15° respectively,
- the missing momentum had either to be smaller than $20 \text{ GeV}/c$ or to have a polar angle between 25° and 155° (to remove most of the $e^+e^- \rightarrow Z\gamma$ events), and
- the invariant mass of the two-jet system had to exceed $40 \text{ GeV}/c^2$.

A kinematic one constraint (1C) fit, requiring the invariant mass of the two-jet system to be either m_W or m_Z , was applied. The input quantities for the fit were the measured vector momenta of the jets. The details of the fitting procedure, namely the errors on the input variables can be found in reference [15].

Four events were found in which the χ^2 of the fit was below 5 when m_{jj} was constrained to be m_W or m_Z . All four candidates have an isolated charged particle with associated electromagnetic energy greater than 20% of its momentum and are thus candidates for the e^* , τ^* , ν_e^* and ν_τ^* channels.

5.2.2 Double production

In double production, the relevant modes are $\ell^*\ell^* \rightarrow \nu\nu WW \rightarrow \nu\nu\ell\nu q_i q_j$, and $\nu^*\nu^* \rightarrow \ell\ell WW \rightarrow \ell\ell\nu\ell q_i q_j$ where, for $m_{\nu^*} \sim m_W$, the leptons from the decay of the excited neutrinos have momenta too low to be selected.

The specific selection criteria were that:

- A_{col} between the jets had to be below 30° ,
- the angle between the isolated particle and the nearest jet had to be above 45° ,
- the missing momentum had to exceed $20 \text{ GeV}/c$.

Five events passed these criteria, while 5.4 ± 0.4 were expected from the SM. The high background is due to the irreducible contribution of the $e^-e^+ \rightarrow WW \rightarrow \ell\nu q_i q_j$ events.

5.3 Hadronic events with two isolated charged particles

Hadronic events with two isolated charged particles (*h220* topology) can result from the single production of excited leptons in the mode $\ell\ell^* \rightarrow \ell\ell Z \rightarrow \ell\ell q_i q_j$, where one of the two final leptons is monochromatic.

The specific selection criteria were that:

- A_{col} and A_{cop} between the jets had to exceed 20° and 10° respectively, and
- the invariant mass of the two jets had to exceed $40 \text{ GeV}/c^2$.

A 5 constraint (5C) kinematic fit, imposing total energy and momentum conservation and constraining the invariant mass of the two-jet system to m_Z , was imposed on the selected events. The input objects for the fit were the two jets and the two isolated leptons. The details of the fitting procedure, namely the errors on the input variables can be found in [15].

No event had a χ^2 per degree of freedom lower than 5, to be compared with the SM expectation of 0.8 ± 0.2 events.

5.4 Leptonic events with charged jets and isolated photons

Leptonic events with one or two charged jets and isolated photons can result from single and double production of excited leptons. The relevant modes are $\ell\ell^* \rightarrow (\ell)\ell\gamma$ and $\ell^*\ell^* \rightarrow \ell\ell\gamma\gamma$, where the spectator lepton can be lost in the t -channel single production mode.

Hard photons are expected in all these channels. Therefore, in the following analysis, only events with at least one isolated photon with an energy greater than 10 GeV were considered.

As stated in [1], the energy can be computed for three- or four-body topologies by imposing energy and momentum conservation and using the polar and azimuthal angles, which are well measured in the detector. This procedure can significantly improve the energy resolution. The method can be applied to tau events since the charged decay products essentially follow the direction of the primary tau.

The compatibility of the momenta calculated from the angles with the measured momenta was quantified on a χ^2 basis. For the charged jets, the χ^2 parameter was defined as

$$\chi_{charged}^2 = \frac{1}{n} \sum_{i=1,n} \left(\frac{p_i^{calc} - p_i^{meas}}{\sigma_i} \right)^2$$

where n is the number of measured charged particles, p_i^{meas} is the measured momentum, p_i^{calc} is the momentum calculated from the kinematic constraints, and σ_i , the quadratic sum of the errors on p_i^{calc} and p_i^{meas} , is defined in reference [1]. For photons, the χ^2 definition was

$$\chi_{photons}^2 = \frac{1}{m} \sum_{i=1,m} \left(\frac{E_i^{calc} - E_i^{meas}}{\sigma_i} \right)^2$$

where m is the number of photons, E_i^{calc} and E_i^{meas} are the calculated and measured electromagnetic energies, respectively, and the error σ_i was taken as just the E_i^{meas} contribution [6] since the E_i^{calc} contribution was estimated to be negligible.

The mass resolution of the lepton-photon pair, after applying the kinematic constraints, is about 1 GeV/ c^2 for electrons and muons and about 2 GeV/ c^2 for taus.

5.4.1 $(\ell)\ell\gamma$ events

This topology ($\ell 101$ and $\ell 102$) selects radiative leptonic events where a hard isolated photon and one charged jet (assumed to be a lepton) were detected. It is relevant to the single production of e^* (spectator electron lost in the beam pipe), and to the single production of μ^* and τ^* when m_ℓ^* is near the kinematic limit. In order to reduce the Compton background [14] drastically and to eliminate Bhabha events where one of the electrons was identified as a photon, the momentum of the charged jet (P_j) had to exceed 10 GeV/ c and the polar angle of the isolated photon had to be between 40° and 140° .

Additional cuts were applied for the electron and muon channels.

In the *electron channel*, events were retained if the electromagnetic energy associated to the charged jet was above $0.2 P_j$, and the angle between the photon and the charged jet was between 100° and 179° . Events with an additional cluster having $\theta < 20^\circ$ or $\theta > 160^\circ$ and an energy lower than the energy of the first cluster were also accepted ($\ell 102$ topology), because these could be events in which the second electron was not properly reconstructed as a charged particle and was therefore detected only by its electromagnetic signature. When there was no additional cluster, it was assumed that the spectator electron was

along the beam direction. In this case the missing energy along the beam direction must be below 30 GeV.

In the *muon channel*, events were retained if the total number of charged particles was less than three, and the charged jet had an associated electromagnetic energy below $0.2 P_j$ and at least one associated hit in the muon chambers.

The events selected in all channels were checked for their coplanarity (the sum of the angles between the particles and the beam direction had to be greater than 355°) and for compatibility between the measured and the calculated momenta (the $\chi^2_{charged}$ had to be less than 5 in the electron and muon channels and the $\chi^2_{photons}$ less than 5 in the tau channel).

Totals of 1, 0 and 2 events with one charged jet and one isolated photon ($\ell 101$ topology) passed all the selection criteria in the electron, muon and tau channels respectively, while 2.8 ± 1.2 , 0.1 ± 0.1 and 1.7 ± 0.8 were expected from the simulation of the SM processes. Two events with one charged jet and two isolated clusters ($\ell 102$ topology) were selected in the electron channel while 5.8 ± 1.6 were expected from the simulation of the SM processes.

5.4.2 $\ell\ell\gamma$ events

This topology ($\ell 201$) selects radiative leptonic events where a hard and isolated photon and two charged jets (assumed to be leptons) were detected.

The $\ell\ell\gamma$ sample was purified by requiring the sum of angles between particles greater than 355° and good agreement ($\chi^2 < 5$) between the measured and calculated values, either for the photons or for the charged leptons. The fact that the condition $\chi^2 < 5$ is not applied simultaneously to the photon and to the charged leptons allows $ee\gamma$ and $\mu\mu\gamma$ events with photons near the borders of the calorimeter modules, where electromagnetic energy can be badly reconstructed, to be kept. In $\tau\tau\gamma$ events, the $\chi^2_{charged}$ is expected to be large because of the missing momenta associated with the neutrinos, and therefore only the measurement of the photon energy is relied upon. The number of events selected after all cuts is 99, while 97.4 ± 6.2 were expected from the SM.

Figure 2(a) shows the invariant mass for the lepton-lepton pairs using the momenta calculated from the kinematic constraint. The two possible $\ell\gamma$ invariant mass combinations are plotted in Fig. 2(b). Figure 2(c) presents the energy and Fig. 2(d) represents the isolation angle of the radiated photon.

The selection criteria were optimized separately for each leptonic channel.

Electron channel

Events were retained if

- they had at least one charged jet with $P_j > 10$ GeV/ c and with associated electromagnetic energy of magnitude greater than $0.2 P_j$,
- the polar angle of the photon was between 40° and 140° ,
- the χ^2 between the jets measured and calculated momenta was smaller than 5.

Muon channel

Events were retained if

- they had two charged jets with associated electromagnetic energy less than 20% of the measured momentum, and at least one with an associated hit in the muon chambers,
- the momentum of the more energetic charged jet was larger than 10 GeV/ c ,

- the polar angle of the photon was between 10° and 170° ,
- the χ^2 between measured and the calculated momenta was smaller than 5 for jets.

Tau channel

Events were retained if

- the polar angle of the photon was between 20° and 160° ,
- the χ^2 between measured and the calculated momenta was greater than 5 for jets and smaller than 5 for the photon.

Totals of 7, 11, and 10 events passed all the selection criteria in the electron, muon and tau channels respectively, while 11.8 ± 2.2 , 7.8 ± 1.8 , and 6.7 ± 1.6 were expected from the simulation of the SM processes.

5.4.3 $\ell\ell\gamma\gamma$ events

This topology ($\ell 202$) selects radiative leptonic events where two hard isolated photons and two charged jets (assumed to be leptons) were detected.

Events were retained if

- the momentum of the lower energy jet was greater than $5 \text{ GeV}/c$,
- at least one of the photons had polar angle between 20° and 160° .

Three events passed these selection criteria while 2.3 ± 1.3 were expected from the simulation of the SM processes.

The hypothesis of double excited lepton production implies the existence in the same event of two $\ell\gamma$ combinations with compatible invariant mass values (the resolution on the mass difference is around $3 \text{ GeV}/c^2$). Only one event fulfills this condition, having $\ell\gamma$ mass combinations of $56.2 \text{ GeV}/c^2$ and $63.8 \text{ GeV}/c^2$. This event has a very small missing energy (3.5 GeV) and one of the charged jets is identified as an electron.

5.5 Leptonic events with charged jets and no isolated photons

Leptonic events with two or more charged jets and no isolated photons can be good candidates for single production of excited leptons in the modes $\ell\ell^* \rightarrow \ell\nu W \rightarrow \ell\nu\nu\ell'$, $\nu\nu^* \rightarrow \nu\ell W \rightarrow \nu\ell\nu\ell'$, $\ell\ell^* \rightarrow \ell\ell Z \rightarrow \ell\ell\nu\nu$, and $\ell\ell^* \rightarrow \ell\ell Z \rightarrow \ell\ell\ell'\ell'$. The selection criteria were optimized separately for events with two or four charged jets.

In events with two charged jets ($\ell 200$), the two jets were required to differ in momentum and not be back-to-back by requiring

- A_{col} and A_{cop} between the jets to be greater than 40° and 25° respectively,
- at least one of the jets to be also identified as an isolated charged particle.

Three events passed all the selection criteria while 1.2 ± 0.3 were expected from the simulation of the SM processes. One of the events had the two jets identified as electrons, one had the two jets identified as muons, and the third had one jet identified as a muon and the other contained three charged particles compatible with a τ decay.

In events with four jets ($\ell 400$), at least two of the jets had to be identified as isolated charged particles. No event passed this selection criterion while 0.1 ± 0.1 were expected from the simulation.

5.6 Photonic events

Final states where the only visible particles are one or two isolated photons can be good candidates for single and double production of excited neutrinos in the modes $\nu\nu^* \rightarrow \nu\nu\gamma$, and $\nu^*\nu^* \rightarrow \nu\nu\gamma\gamma$. Such channels are also relevant in the search for neutralino production [16].

An analysis dedicated to the single photon channel ($\ell 001$) was performed with the same selection criteria as described in reference [4], except that the minimal photon energy required for a single photon was 4.0 GeV. Eleven events were selected as having a single γ in the barrel region (i.e. $\theta_\gamma = 45^\circ - 135^\circ$). None of these had $E_\gamma > 60$ GeV. From the SM reaction $e^+e^- \rightarrow \gamma\nu\bar{\nu}$, 14.4 events were expected above 4 GeV and 0.13 above 60 GeV. The single photon trigger efficiency was estimated to be greater than 85%.

In the two photon channel ($\ell 002$), the two photons must have high energy and be acollinear and acoplanar. The $\gamma\gamma(\gamma)$ data sample was selected by requiring no charged particles and moreover imposing the following criteria.

- There had to be at least two electromagnetic energy depositions with more than 10 GeV (one being more than 20 GeV) and obeying the following acceptance criteria:
 - the polar angle had to be between 25° and 35° or 145° and 155° or between 42° and 88° or 92° and 138° , where the polar angle lower limit is defined to reduce the Bhabha background drastically and provide a high TPC efficiency;
 - the azimuthal angle Φ , modulo 60° , had to be outside $30^\circ \pm 2.5^\circ$ for the barrel depositions and $30^\circ \pm 3.0^\circ$ for the forward ones in order to avoid the boundaries between TPC sectors and ensure a high intrinsic efficiency for detecting and reconstructing any charged particle in the TPC;
 - the angle between the two photons had to be greater than 30° .
- Events with hadronic clusters greater than 3 GeV, not associated to photons, were rejected if less than 90% of the energy was deposited in the first layer of the hadron calorimeter. This selection eliminated most cosmic ray events.

No attempt was made to recover photons converted by the material in DELPHI before the TPC. The trigger efficiency was greater than 95%. 47 events were selected. The acoplanarity of these events is shown in Fig. 3. None had an acoplanarity greater than 10° . From the QED background reaction $e^+e^- \rightarrow \gamma\gamma$, 48.0 ± 2.0 events were expected in total, but only 0.05 ± 0.03 events were expected with an acoplanarity above 10° .

6 Results and limits

The search for the production of excited leptons involved many final states. For each excited lepton, the weight of each possible final state depends, as discussed in section 2, on the decay branching ratios which are functions of the excited lepton mass and of the coupling parameters.

The numbers of events that survived the cuts defined in the previous section, as well as the numbers expected from the simulation, are summarized in tables 2 and 3 as a function of the excited lepton flavour and production mode. In the cases where no flavour selection was possible (for instance in the *hadronic* events with no isolated particles), the same event contributes to all possible flavours.

Events in which the excited lepton mass could not be estimated were treated as candidates for all values of the mass. However, the possible invariant masses can be deduced in topologies with isolated leptons or photons.

Topology	e^*			μ^*			τ^*		
	$e\gamma$	νW	eZ	$\mu\gamma$	νW	μZ	$\tau\gamma$	νW	τZ
$h200$	-	2 (5.1)	-	-	2 (5.1)	-	-	2 (5.1)	-
$h210$	-	4 (3.7)	4 (3.5)	-	0 (0.5)	0 (0.4)	-	4 (7.5)	4 (7.2)
$h220$	-	-	0 (0.8)	-	-	0 (0.8)	-	-	0 (0.8)
$\ell101$	1 (2.8)	-	-	0 (0.1)	-	-	2 (1.7)	-	-
$\ell102$	2 (5.8)	-	-	-	-	-	-	-	-
$\ell201$	7 (11.8)	-	-	11 (7.8)	-	-	10 (6.7)	-	-
$\ell200$	-	1 (0.6)	-	-	1 (0.6)	-	-	3 (1.2)	-
$\ell400$	-	-	0 (0.1)	-	-	0 (0.1)	-	-	0 (0.1)
$h210$	-	5 (5.4)	-	-	5 (5.4)	-	-	5 (5.4)	-
$\ell202$	1 (0.4)	-	-	0 (0.4)	-	-	0 (0.4)	-	-

Table 2: Number of candidates for each excited charged lepton and each decay mode ($\ell\gamma$, νW or ℓZ) as a function of the detected final state topology. The corresponding SM expectations are indicated in parentheses. The topology is indicated in the first column as $xijk$, where x is h or ℓ for *hadronic* or *leptonic* events and i , j , and k represent respectively the number of jets, the number of isolated charged particles, and the number of photons. These candidates were selected for single production of ℓ^* except for the last two topologies, which refer to the double production of ℓ^* .

In *leptonic* events with isolated photons, the possible invariant masses of excited leptons are given simply by the invariant masses of all lepton-photon combinations. The mass resolution of the lepton-photon pair, after applying the kinematic constraints, is about $1 \text{ GeV}/c^2$ for electrons and muons and about $2 \text{ GeV}/c^2$ for taus.

In *hadronic* events with one isolated lepton, the lepton can either be the spectator lepton (as for instance in $\ell\ell^* \rightarrow \ell\nu W \rightarrow \ell\nu q_i q_j$) or can originate from the excited lepton decay (as for instance in $\nu\nu^* \rightarrow \nu\ell Z \rightarrow \nu\ell q_i q_j$).

If the lepton is the spectator lepton, the mass of the excited lepton can be deduced from the measured lepton momentum (P_ℓ) by conservation of energy and momentum (ie from $m_\ell^2 = s - 2 k P_\ell \sqrt{s}$), where k is 1.0 for electrons and muons and 1.4 for taus to take in account the missing energy in tau decay). The mass resolution is about $1 \text{ GeV}/c^2$ for muons, $1.5 \text{ GeV}/c^2$ for electrons and $2.5 \text{ GeV}/c^2$ for taus.

Topology	ν_e^*			ν_μ^*			ν_τ^*		
	$\nu\gamma$	ℓW	νZ	$\nu\gamma$	ℓW	νZ	$\nu\gamma$	ℓW	νZ
$h200$	-	2 (5.1)	2 (5.1)	-	2 (5.1)	2 (5.1)	-	2 (5.1)	2 (5.1)
$h210$	-	4 (3.7)	-	-	0 (0.5)	-	-	4 (7.5)	-
$\ell200$	-	3 (1.2)	-	-	3 (1.2)	-	-	3 (1.2)	-
$\ell001$	0 (0.13)	-	-	0 (0.13)	-	-	0 (0.13)	-	-
$h210$	-	5 (5.4)	-	-	5 (5.4)	-	-	5 (5.4)	-
$\ell002$	0 (0.05)	-	-	0 (0.05)	-	-	0 (0.05)	-	-

Table 3: As Table 2, but for excited neutrinos instead of excited charged leptons.

If the detected lepton comes from the decay of the excited lepton, the excited lepton mass can be obtained from the invariant mass of the $\ell jetjet$ system after applying the fit procedure described in section 5.2. The hypothesis that the $jetjet$ system originated from a W or a Z decay was tested according to the decay mode studied. The ℓ^* mass resolution is about $5 \text{ GeV}/c^2$ for e and μ and $15 \text{ GeV}/c^2$ for τ .

In *hadronic* events with two isolated leptons, one of the leptons must be the spectator and the $jetjet$ system must come from a Z decay. Both hypotheses were tested. The mass resolution is about $1 \text{ GeV}/c^2$ for muons and $1.5 \text{ GeV}/c^2$ for electrons.

Decay mode	e^*	μ^*	τ^*	ν_e^*	ν_μ^*	ν_τ^*
$\ell\gamma$	42	67	37	-	-	-
νW	35	55	50	-	-	-
ℓZ	19	45	15	-	-	-
$\nu\gamma$	-	-	-	47	47	47
ℓW	-	-	-	31	37	20
νZ	-	-	-	35	35	35
$\ell\gamma$	47	50	40	-	-	-
νW	16	16	16	-	-	-
$\nu\gamma$	-	-	-	36	36	36
ℓW	-	-	-	18	18	18

Table 4: Efficiencies (in %) for each excited lepton (e^* , μ^* , τ^* , ν^*) for each decay mode (γ , Z or W). The efficiencies are calculated for single production of ℓ^* with $m_{\ell^*} = 150 \text{ GeV}/c^2$ except for the last four lines, where double production of ℓ^* with $m_{\ell^*} = 75 \text{ GeV}/c^2$ is considered.

The efficiencies for each excited lepton (e^* , μ^* , τ^* , ν^*) for each decay mode (γ , Z or W), in the single and the double production cases, are given in table 4 for chosen m_{ℓ^*} values. The trigger efficiency is included. The dependence of efficiency on m_{ℓ^*} is weak, because of the combination of the several topologies studied. For the W decay of the excited neutrino, only final states with two jets and one isolated charged particle were considered because the other topologies ($h200$ and $\ell200$) do not contribute to improving the limits due to the low efficiency and to the high background due to the impossibility of reconstructing the ν^* mass.

The global efficiency for each excited lepton was then calculated, using the decay branching ratios corresponding to particular cases of the coupling parameters f and f' (see section 2).

The upper limits at 95% confidence level on the ratio λ/M_{ℓ^*} (see section 2.1), obtained in the single production modes, are a function of the ℓ^* mass. The limits were calculated using a Poisson distribution with background. Figs. 4 and 5 show these limits for $f = f'$ and $f = -f'$ respectively. These limits include the results of the previous analysis at a centre-of-mass energy of 130-136 GeV [1]. The new data extend the mass region explored up to 161 GeV.

The lower limits at 95% of confidence level on the excited charged lepton masses, obtained in the double production modes, are given in table 5, both for $f = f'$ and for $f = -f'$, and in both cases for the assumption that they have left-handed couplings

Lower limit	$f = f'$	$f = -f'$
e^*	79.6 (77.9)	70.9 (44.6)
μ^*	79.6 (78.4)	70.9 (44.6)
τ^*	79.4 (77.4)	70.9 (44.6)
ν^*	56.4 (44.9)	77.6 (64.4)

Table 5: Lower limits (in GeV/ c^2) at 95 % confidence level on the excited lepton mass from the double production modes. The first values are obtained assuming both left and right-handed components, while the values in parentheses consider conservatively only left-handed components.

only (given in parentheses), as well as for the assumption that they have both left and right-handed couplings.

7 Conclusions

DELPHI data corresponding to a total luminosity of 10 pb $^{-1}$ at a centre-of-mass energy of 161 GeV have been analysed, searching for radiative decays of charged and neutral excited leptons involving γ , Z or W emission. No significant signal was observed.

The search for double production of excited leptons gave the excited lepton mass limits shown in Table 5. The search for single production gave the limits on the ratio λ/m_ℓ^* shown in Fig. 4 and 5. These results considerably extend the limits set recently from the run of LEP at centre-of-mass energies of 130 – 136 GeV or previously at LEP1 and HERA [1,2].

Acknowledgements

We would like to thank J.L.Kneur for the very useful discussions on the excited lepton production. We are greatly indebted to our technical collaborators and to the funding agencies for their support in building and operating the DELPHI detector, and to the members of the CERN-SL Division for the excellent performance of the LEP collider.

References

- [1] DELPHI Coll., P. Abreu et al., Phys. Lett. **B380** (1996) 480;
DELPHI Coll., P. Abreu et al., Zeit. Phys. **C53** (1992) 41.
- [2] ALEPH Coll., D. Decamp et al., Phys. Lett. **B385** (1996) 445;
ALEPH Coll., D. Decamp et al., Phys. Lett. **B250** (1990) 172;
H1 Coll., I. Abt et al., Nucl. Phys. **B396** (1993) 3;
L3 Coll., M. Acciarri et al., Phys. Lett. **B370** (1996) 211;
L3 Coll., B. Adeva et al., Phys. Lett. **B247** (1990) 177;
Phys. Lett. **B250** (1990) 205; Phys. Lett. **B252** (1990) 525;
OPAL Coll., G. Alexander et al., Phys. Lett. **B386** (1996) 486;
OPAL Coll., M.Z. Akrawy et al., Phys. Lett. **B257** (1991) 531;
ZEUS Coll., M. Derrick et al., Z. Phys. **C65** (1994) 627.
- [3] K. Hagiwara, S. Komamiya, D. Zeppenfeld, Z. Phys. **C29** (1985) 115.
- [4] DELPHI Coll., P. Abreu et al., Phys. Lett. **B380** (1996) 471.
- [5] F. Boudjema, A. Djouadi and J.L. Kneur, Z. Phys. **C57** (1993) 425.
- [6] DELPHI Coll., P. Aarnio et al., Nucl. Instr. Methods **A303** (1991) 233;
DELPHI Coll., P. Abreu et al., Nucl. Instr. Methods **A378** (1996) 57.
- [7] T. Sjöstrand, Comp. Phys. Comm. **82** (1994) 74;
T. Sjöstrand, Pythia 5.7 and Jetset 7.4, CERN-TH/7112-93.
- [8] F.A. Berends, R. Pittau, R. Kleiss, Comp. Phys. Comm **85** (1995) 437.
- [9] S. Nova, A. Olchevski and T. Todorov, “TWOOGAM, a Monte Carlo event generator for two photon physics”, DELPHI Note 90-35 PROG 152.
- [10] F.A. Berends, P.H. Daverveldt, R. Kleiss, Comp. Phys. Comm. **40** (1986) 271.
- [11] D. Karlen, Nucl. Phys. **B289** (1987) 23.
- [12] F. Berends and R. Kleiss, Nucl. Phys. **B186** (1981) 22.
- [13] S. Catani et al., Phys. Lett. **B269** (1991) 432.
- [14] Min-Shih Chen, P. Zerwas, Phys. Rev. **D12** (1975) 187.
- [15] N. Kjaer and R. Moller, “Reconstruction of invariant masses in multi-jet events”, DELPHI Note 91-17 PHYS 88.
- [16] DELPHI Coll., “Search for charginos, neutralinos and gravitinos at LEP”, in preparation.

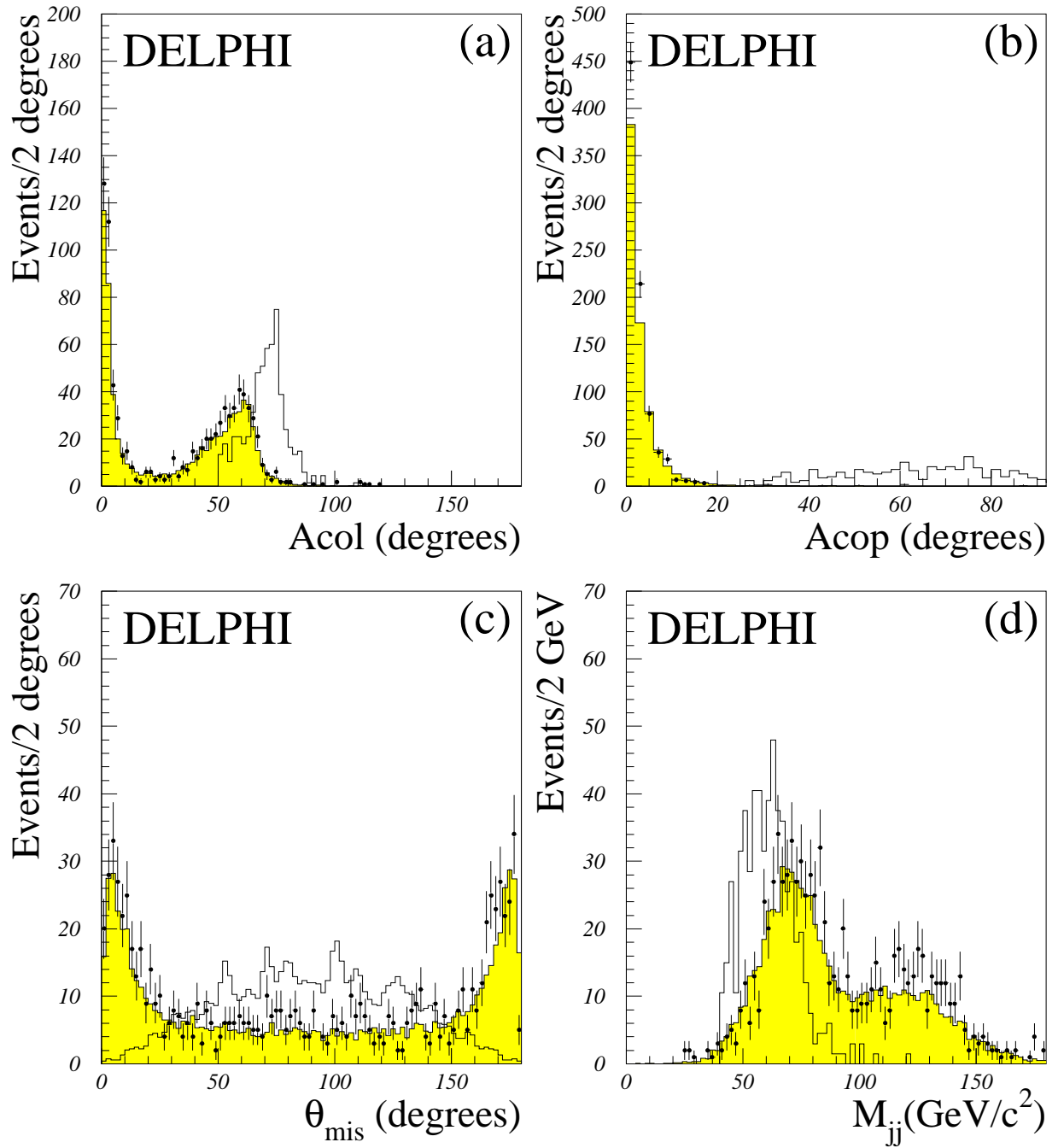


Figure 1: The acollinearity (a) and acoplanarity (b) between the two jets, polar angle of the missing momentum (c), and invariant mass of the two jets (d), for the sample of *hadronic* events with no isolated particles. The dots show the data and the shaded histogram shows the SM simulation. The other histogram shows a typical signal simulation with arbitrary normalization.

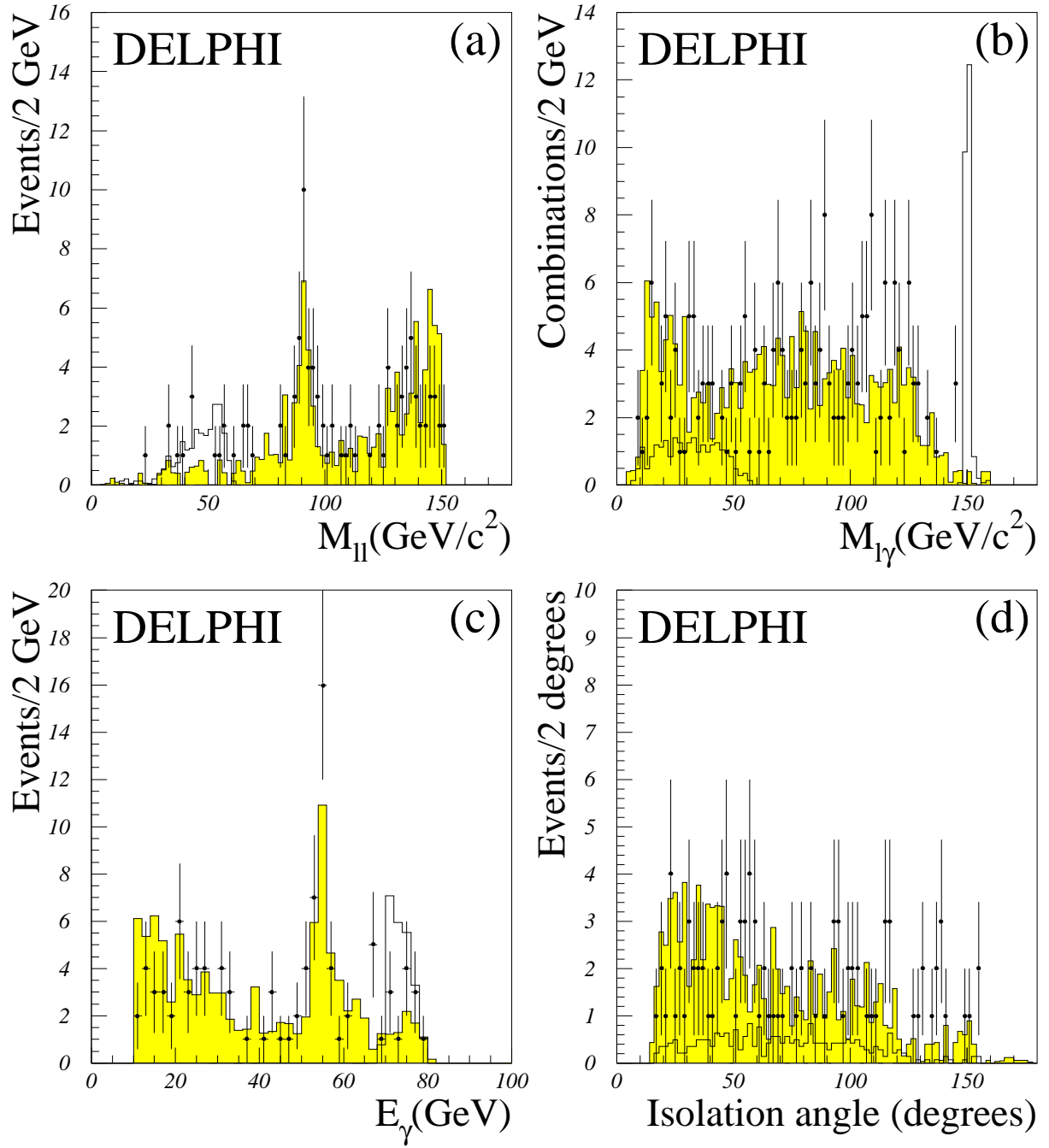


Figure 2: Invariant mass of the two leptons (a), invariant mass of lepton-photon pairs (b), and energy (c) and isolation angle (d) of the photon, for the $ll\gamma$ sample. The dots show the data and the shaded histogram shows the SM simulation. The other histogram shows a typical signal simulation with arbitrary normalization.

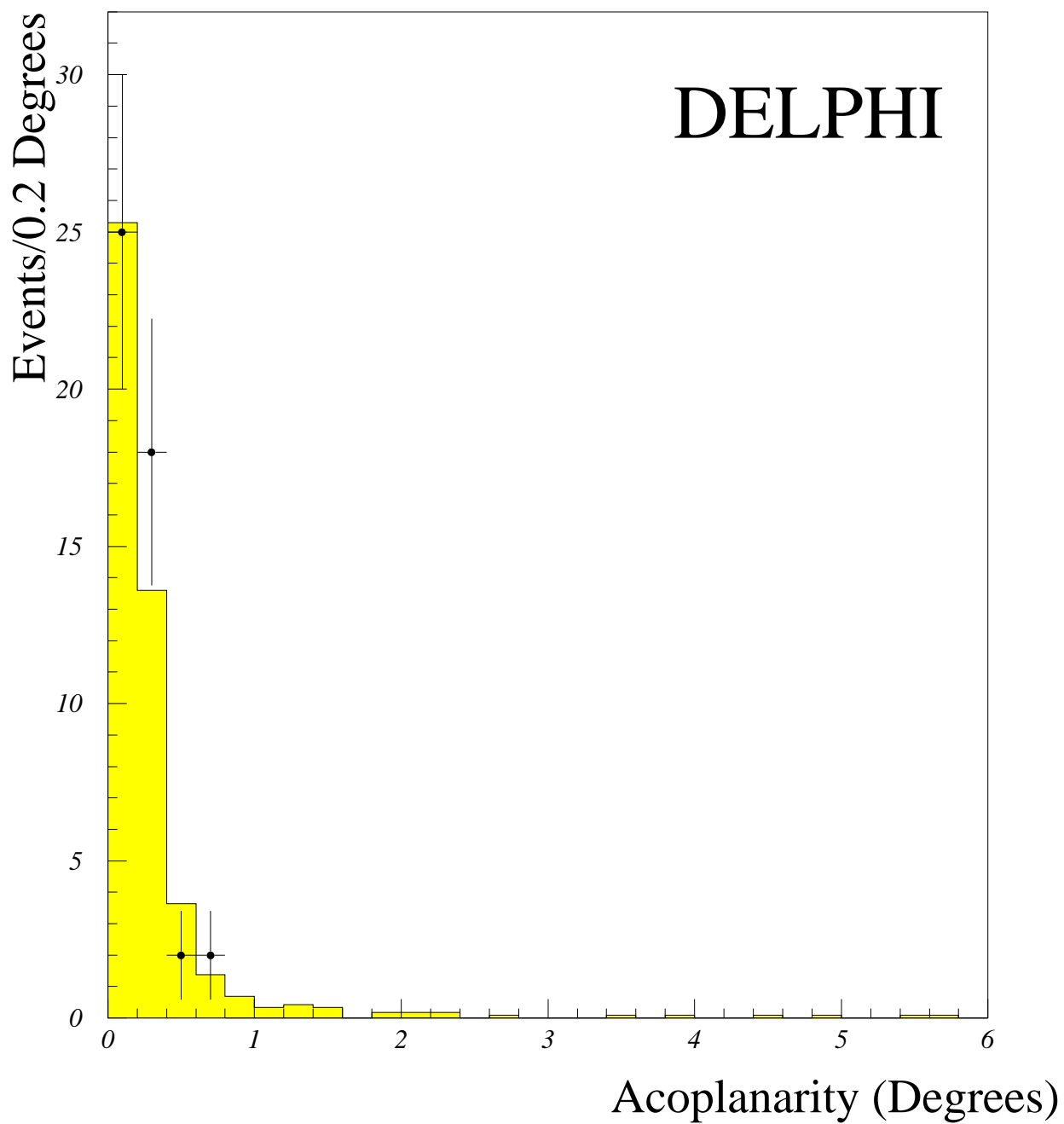


Figure 3: Acoplanarity of the two photons for the $\gamma\gamma$ sample. The dots show the data and the shaded area shows the SM simulation.

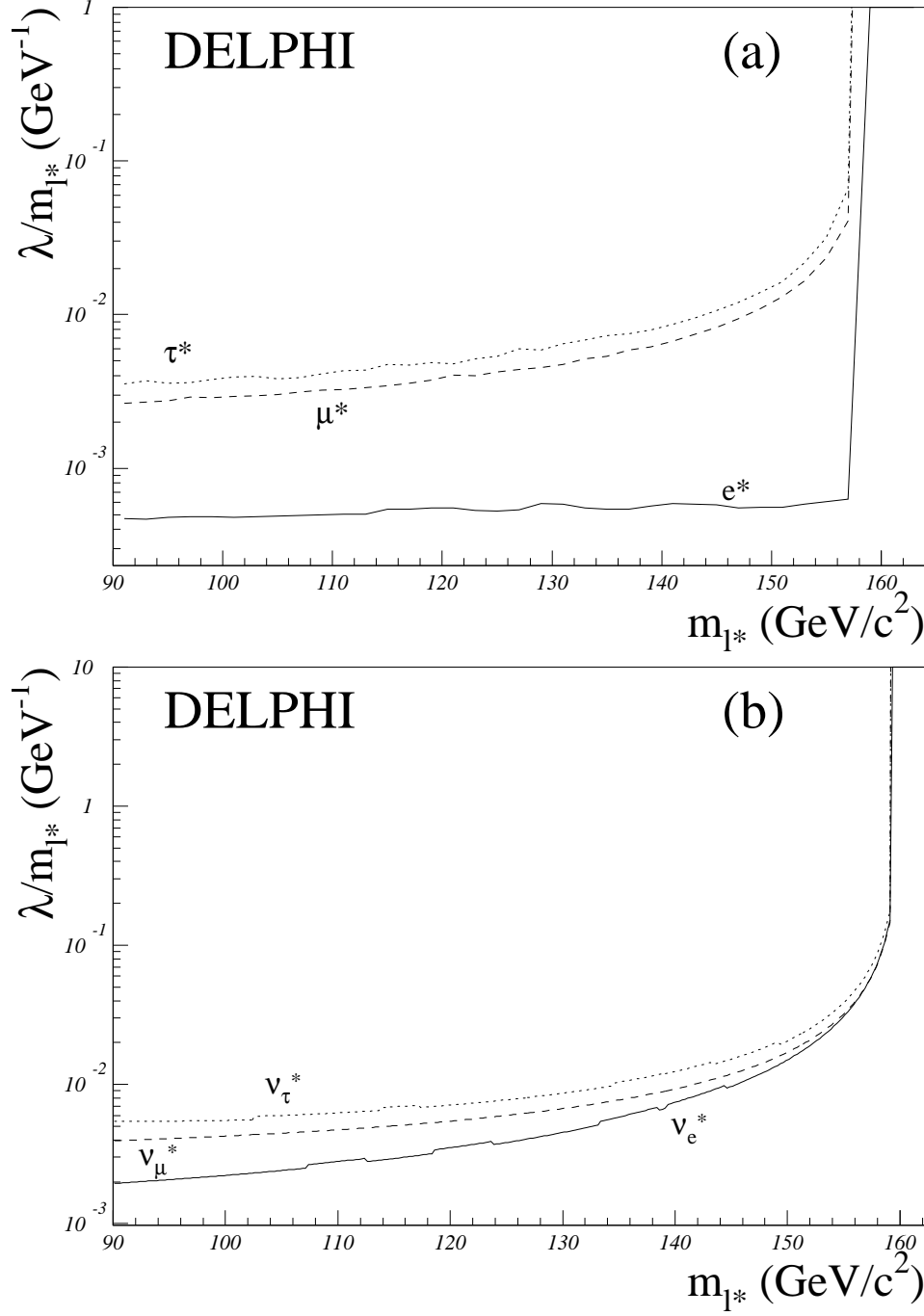


Figure 4: Results on single production of excited charged (a) and neutral (b) leptons assuming $f = +f'$. The line shows the upper limits at 95% confidence level on the ratio λ/m_{l^*} between the coupling of the excited charged lepton and its mass as a function of its mass.

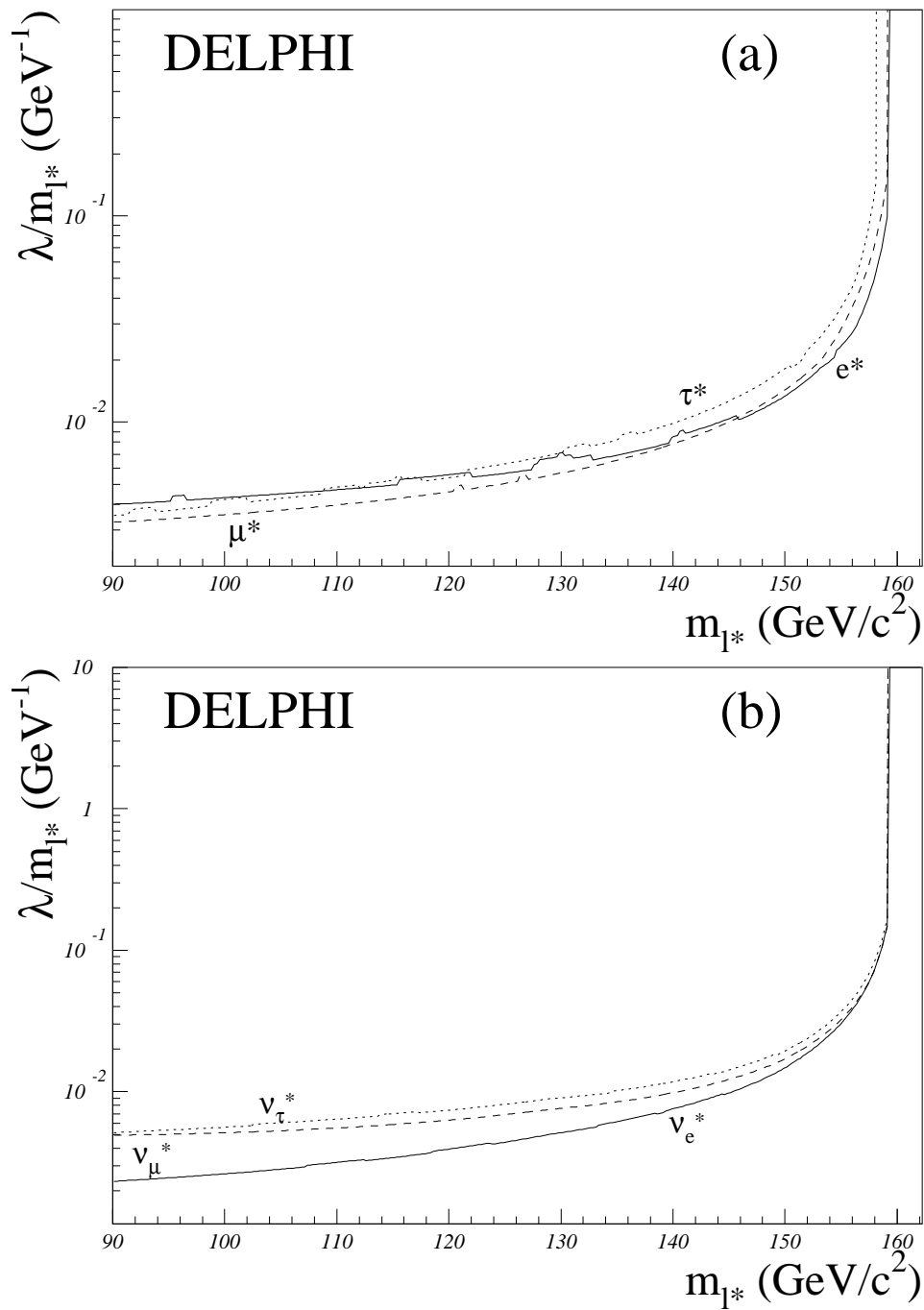


Figure 5: As Fig. 4, but for $f = -f'$.